PERGAMON

PII: S1359-6454(98)00407-8

Acta mater. Vol. 47, No. 4, pp. 1297–1305, 1999

Printed in Great Britain
1359-6454/99 $19.00 + 0.00

SPALLING FAILURE OF A THERMAL BARRIER COATING ASSOCIATED WITH ALUMINUM DEPLETION IN THE BOND-COAT

E. A. G. SHILLINGTON and D. R. CLARKE†

Materials Department, College of Engineering, University of California, Santa Barbara, CA 93106-5050, U.S.A.

(Received 16 June 1998; accepted 23 November 1998)

Abstract—A plasma-sprayed thermal barrier coating is observed to spall after oxidation at 1121°C from a CoNiCrAlY bond-coated superalloy at the interface between the thermally grown oxide (TGO) and the zirconia thermal barrier coating (TBC). Phase characterization by photostimulated luminescence and X-ray diffraction, as well as microstructural characterization by scanning electron microscopy, indicates that the spalling is associated with the conversion of the initially formed α-alumina thermally grown oxide to α-chromia and a (CoNi)(CrAl) spinel. It is proposed that the phase conversion occurs after the alumina TGO has cracked on thermal cycling and the underlying bond-coat alloy is depleted of aluminum with concurrent enrichment of the oxide by Cr, Co and Ni. The observations suggest that monitoring the luminescence intensity as a function of oxidation time might form the basis of a nondestructive tool for detecting the onset of failure based on the disappearance of α-alumina. © *1999 Acta Metallurgica Inc. Published by Elsevier Science Ltd. All rights reserved.*

1. INTRODUCTION

Although thermal barrier coatings (TBCs) are already being widely used in a variety of gas turbine and diesel engine applications, greater benefits are expected to accrue with TBCs that can be used in critical applications, namely those in which a loss of the coating would expose the underlying metal to a temperature in excess of its design specifications. This requires an increase in the reliability of the coatings particularly with regard to failure by spalling since the TBCs are usually under biaxial compression, as a result of the smaller coefficient of thermal expansion of most TBCs compared with the underlying metal.

Considerable increases in the reliability of TBCs have come from improvements in the processes used for deposition, in large part because of improvements in coating consistency. However, one of the difficulties in choosing a combination of alloy/bond-coat/TBC for improved reliability is that the mechanisms by which TBCs spall have not been fully identified. There is an additional complication in that there is circumstantial evidence to suggest that different failure mechanisms pertain in the failure of TBCs deposited by electron beam evaporation and plasma-spraying. This is further complicated by the fact that plasma-sprayed coated materials tend to be used at lower temperatures than those deposited by electron beam evaporation. In this work we present experimental observations suggesting that one failure mode is associated with a compositional change in the thermally grown oxide from alumina to a mixture of chromia and spinel, and that this is, in turn, associated with depletion of Al from the bond-coat and concurrent enrichment of Co, Ni and Cr in the oxide. Failure of alumina scales on overlay oxidation coatings has previously been associated with aluminum depletion effects [1–3] and it has recently been implicated in the failure of TBCs on a MCrAlY bond-coat [4].

The coated system investigated in this work was an IN939 superalloy with a MCrAlY (CT102) bond-coat of nominal composition 38Co–32Ni–21Cr–8Al–0.8Y (wt%) and a plasma-sprayed thermal barrier coating of nominal composition ZrO_2–9% Y_2O_3. For purposes of evaluating the dependence of the thickness of the TBC coating on the residual stress, the TBC had been polished at an angle of 1:100 to produce a gradient in TBC thickness across the sample as well as to expose the bond-coat on one side. The sample is shown in the optical micrograph of Fig. 1, with the exposed bond-coat at the left-hand side. (The vertical bands correspond to different thicknesses of the TBC and the dark, circular dot is a hole drilled in the specimen so as to suspend it in the furnace during oxidation.)

†To whom all correspondence should be addressed.

2. RESIDUAL STRESS EVOLUTION ON OXIDATION

The specimen was oxidized in air at 1121°C for successively longer periods of time (1, 2, 4, 8, 16, 32 h). After each oxidation the sample was cooled to room temperature and the photostimulated Cr^{3+} fluorescence (luminescence) spectrum recorded. The luminescence was studied as both a probe for the presence of α-alumina and the piezospectroscopic measurement of residual stress in the oxide formed at the interface between the TBC and the bond-coat alloy. The experimental procedure and the data analysis have been described previously [5–8]. The nominal compressive stress was determined from the observed frequency using the phenomenological equation:

$$\Delta\nu_{\text{stress}} = \Pi_{ij}\sigma^{c}_{ij} = \Pi_{ij}a_{ki}a_{lj}\sigma_{kl} \tag{1}$$

where Π_{ij} is the ijth component of the piezospectroscopic tensor and σ^{c}_{ij} the stress state in the crystallographic basis of the host crystal. (The Einstein summation convention is assumed.) In a general coordinate system, the stress state, σ_{ij}, is related to σ^{c}_{ij} by the transformation matrix, a_{ij}. Because the off-diagonal terms of the piezospectroscopic tensor are nearly zero for alumina [9], equation (1) may be substantially reduced:

$$\Delta\nu_{\text{stress}} = \Pi_{ii}\sigma_{jj} - [\Pi_a(a_{i2}a_{j2} + a_{i3}a_{j3}) + \Pi_m(a_{i1}a_{j1} + a_{i3}a_{j3}) + \Pi_c(a_{i1}a_{j1} + a_{i2}a_{j2})]\sigma_{ij} \tag{2}$$

where the subscripts a, m and c refer to the respective crystallographic directions in the corundum structure. For an untextured polycrystalline material, provided the volume probed by the exciting laser beam is large compared to the grain size, the piezospectroscopic shift can be shown to depend only on the hydrostatic component of the stress:

$$\overline{\Delta\nu} = \frac{1}{3}\Pi_{ii}\sigma_{jj} \tag{3}$$

where equation (3) is obtained by averaging equation (2) over all spatial orientations. For oxide scales having no crystallographic texture, the stresses can be assumed to be equi-biaxial, such that $\sigma_{xx} = \sigma_{yy} = \bar{\sigma}$ and $\sigma_{zz} = 0$. In this limit, equation (3) reduces to

$$\overline{\Delta\nu} = \frac{2}{3}\Pi_{ii}\bar{\sigma} \tag{4}$$

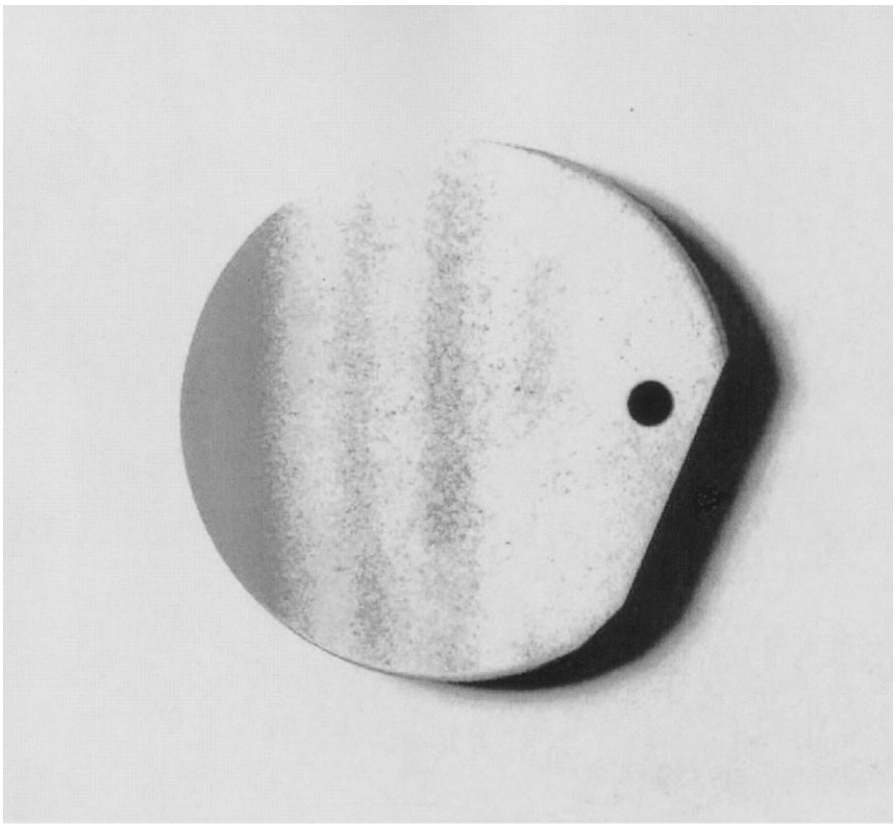

Fig. 1. Optical micrograph of the plasma-sprayed TBC after taper polishing the TBC so that the bond-coat is exposed at the left-hand side. (The hole is used to suspend the sample in the oxidation furnace.)

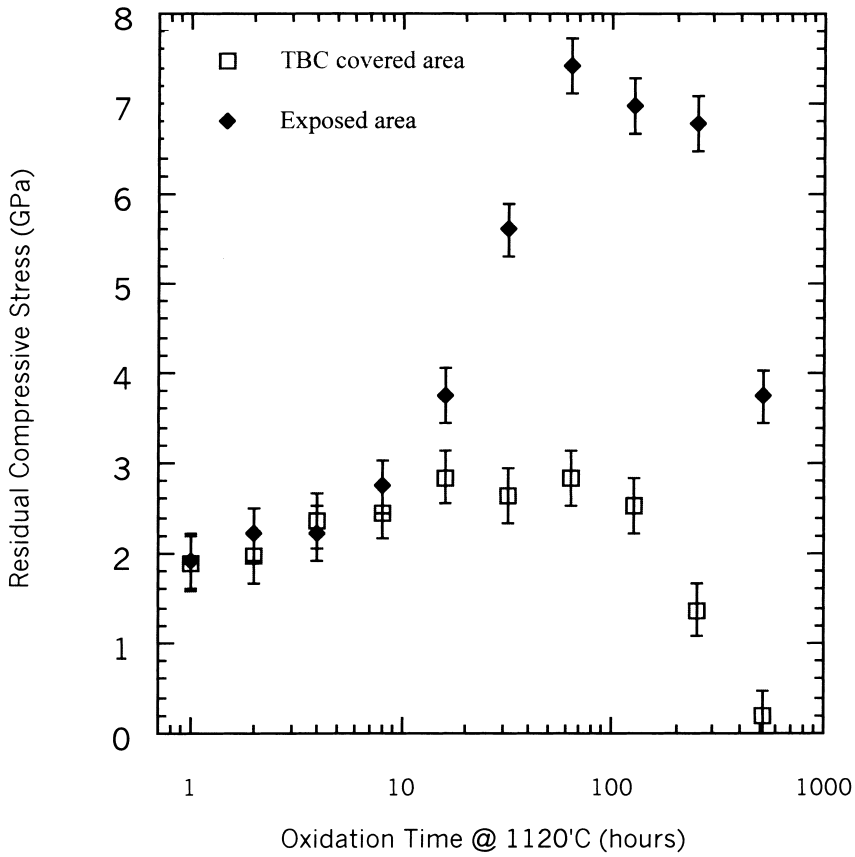

Fig. 2. The nominal biaxial compressive residual stress in the thermally grown alumina as a function of oxidation time at 1121°C. The stresses were calculated from the measured frequency shift of the R2 fluorescence line using equation (4) in the text.

where $\bar{\sigma}$ is the net effect of the growth stresses established at the oxidation temperature and the thermal expansion mismatch stress arising upon cooling. The experimentally measured value of Π_{ii} is 7.60 cm^{-1}/GPa for both of the ruby lines [9]. The term, nominal compressive stress, is used since the relationship of equation (1) assumes that the oxide is formed on a flat surface. When the surface is not flat, the determination of the residual stress state from the observed frequency shift requires a detailed and quantitative knowledge of the surface roughness [10]. (The same proviso of course, pertains to the interpretation of residual stress from X-ray diffraction measurements [10].)

Not normally considered is that changes in chromium concentration in the α-alumina also cause a shift in the characteristic luminescence lines. According to Kaplyanskii *et al.* [11], the frequency shift varies linearly with chromium concentration, c_m, as $\Delta\nu = 0.99c_m$, so increasing chromium concentration has the same effect as decreasing hydrostatic stress.

Since the bond-coat was exposed in polishing the wedge, both thermally grown oxide on the bare bond-coat as well as under the TBC could be probed after each oxidation exposure. The evolution of the nominal compressive stress in the thermally grown oxide is shown in Fig. 2. (Note, the oxidation time is plotted on a logarithmic scale.) The stress under the TBC builds up slowly with time for the first 10 h and then remains almost constant at about 2.5 GPa up to about 128 h. In this respect it behaves in a similar manner to the stress evolution on the same bond-coat under an EB-PVD coating. In contrast, the compressive stress in the thermally grown oxide on the polished bond-coat surface continued to increase up to a maximum of about 7.5 GPa. The higher value of the nominal stress on the polished bond-coat than under the TBC is attributed to the fact that the bond-coat is rough under the TBC and so it is not in a state of biaxial compression as it is on the polished surface. As a result, there are out-of-plane stresses in the thermally grown oxide and so the simple relation of equation (4) cannot strictly be used. Nevertheless, for comparison purposes, as is done in this work, it is used. (The effect of sinusoidal roughness is to decrease the observed frequency shift [10] but without quantitative knowledge of the detailed geometry of the roughness of the coating, the actual stress in the alumina cannot be determined.)

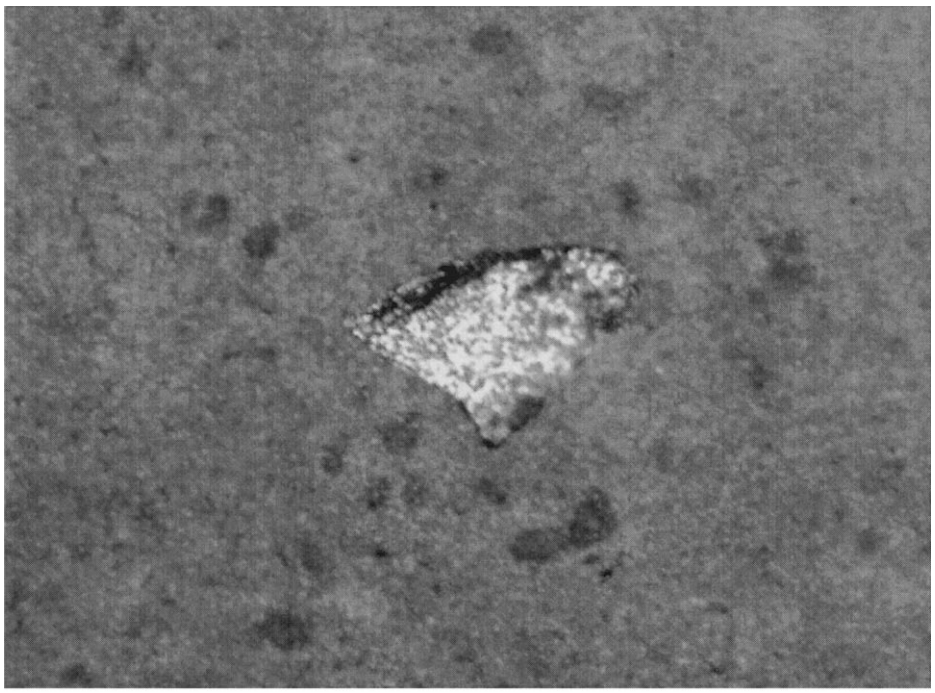

Fig. 3. An example of the occasional localized spalling noted after oxidation. The spalling in these cases occurs at the interface with the bare bond-coat as indicated by the specular optical reflection from these regions and the absence of any luminescence.

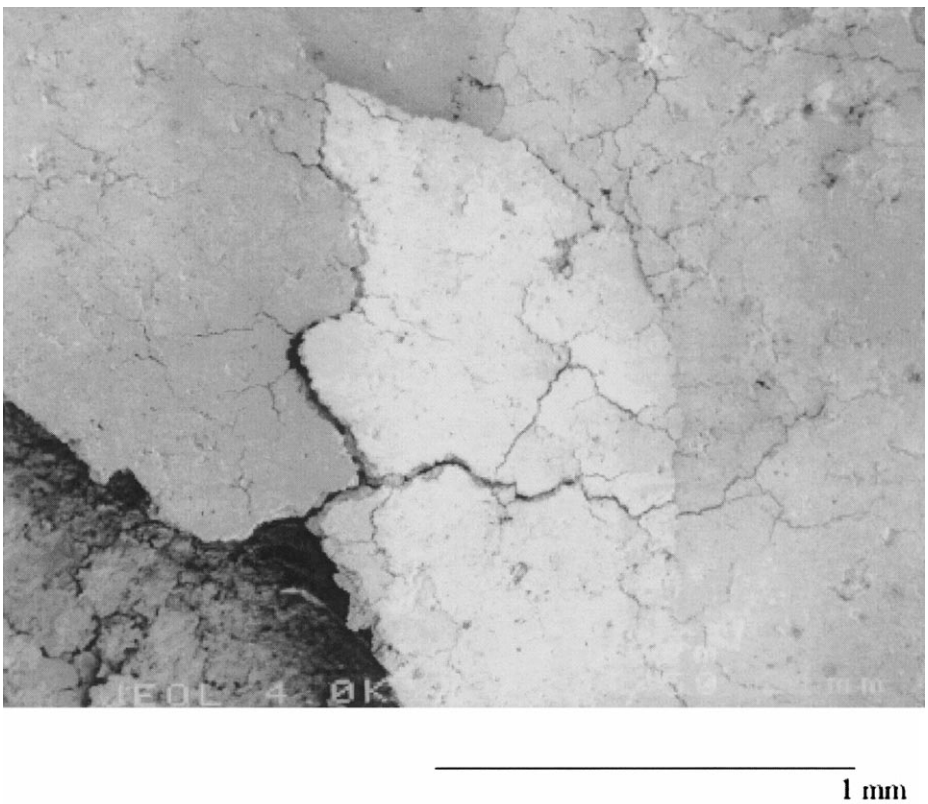

Fig. 4. The surface of the small region of still adhering TBC after the majority of the TBC had spalled away. Extensive cracking and buckling of the TBC is apparent. Scanning electron micrograph.

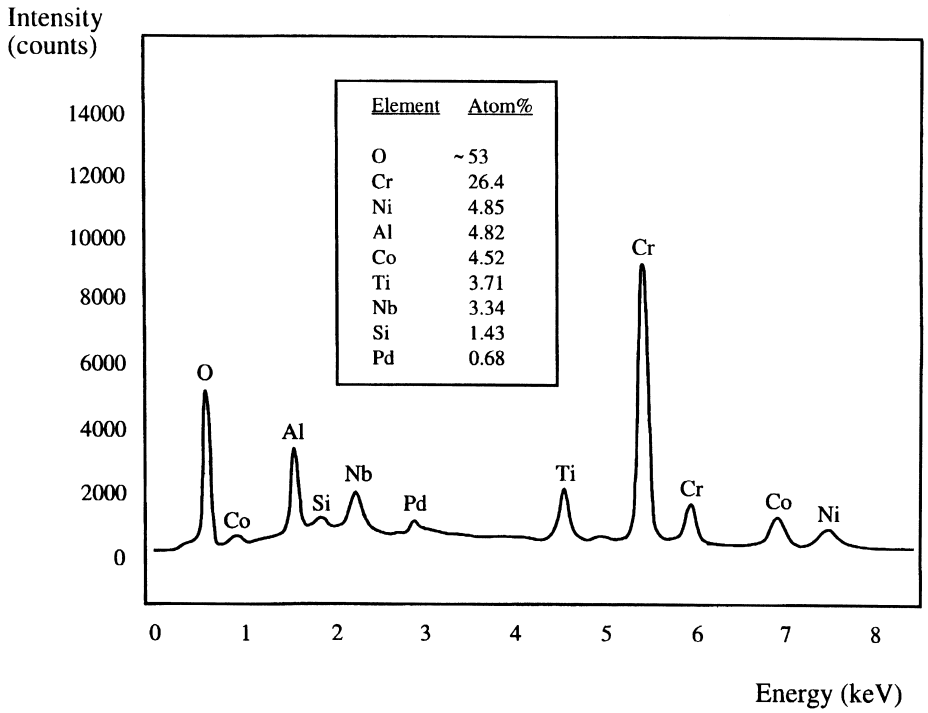

Fig. 5. Energy dispersive X-ray spectrum recorded from the bond-coat surface exposed by spalling.

Then, with subsequent oxidation after 128 h the frequency shift, and hence the nominal compressive stress, began to decrease in magnitude on both the polished bond-coat surface and under the thermal barrier coating, as shown by the data in Fig. 2. In addition, small isolated spalls, such as shown in the photomicrograph of Fig. 3, also began to occur after 128 h with the spalling occurring at the bond-coat/TGO interface exposing the bare metal. Finally, after a total of 512 h oxidation at 1121°C, most of the TBC spalled, in one piece, from the bond-coat on cooling. The spalled piece was preserved for analysis as was the bond-coat surface exposed by the spalling.

3. POST-SPALLING CHARACTERIZATION

Although most of the TBC had spalled away, a small region remained adhered to the specimen. The intensity of the fluorescence was very low, almost two orders of magnitude smaller than that from the coating after 128 h. In addition, the nominal compressive stress determined from the luminescence frequency was almost zero (Fig. 2). Examination of both the bond-coat surface exposed by the spalling and the underside of the spalled TBC revealed that fluorescence was only obtained from small isolated patches, a few microns across, suggesting that little α-alumina remained on either the bond-coat or the TBC surfaces.

The adhered piece of the TBC and the bond-coat surface exposed by the spalling were examined using scanning electron microscopy. As shown in Fig. 4, the adhered TBC was extensively cracked and appeared to have buckled. Scanning microscopy of the exposed bond-coat surface was not useful in identifying the nature of the surface but EDAX analysis of the surface revealed a high concentration of Cr and only comparatively low concentrations of Al, Co, Ni, Ti and Nb (Fig. 5). X-ray diffraction analysis of the surface, Fig. 6, revealed a much more complex picture indicating mainly Cr_2O_3 and a spinel phase, possibly a (Co,Ni)(Cr,Al) spinel, as well as the presence of weaker peaks of Al_2O_3 and zirconia and rutile. The X-ray diffraction analysis identification of chromia, spinel and the other phases was thus consistent with there being little detectable fluorescence from α-Al_2O_3 over most of the surface. Interestingly, the lattice parameters, determined from the X-ray diffraction peaks, of both the α-Cr_2O_3 and the remaining α-Al_2O_3 corresponded to that of the bulk, unstrained oxides.

4. PHASE EVOLUTION IN THE THERMALLY GROWN OXIDE

In order to elucidate the changes in the thermally grown oxide during oxidation a series of experiments were performed to characterize the phases and their spatial distribution at different oxidation times. Pieces of the same bond-coated alloy were oxidized for different times (64, 128, 256, 384, 512 and 640 h) at 1121°C and the plasma-sprayed coating was then pried from the samples to facilitate X-ray diffraction of the oxide. They were then cross-

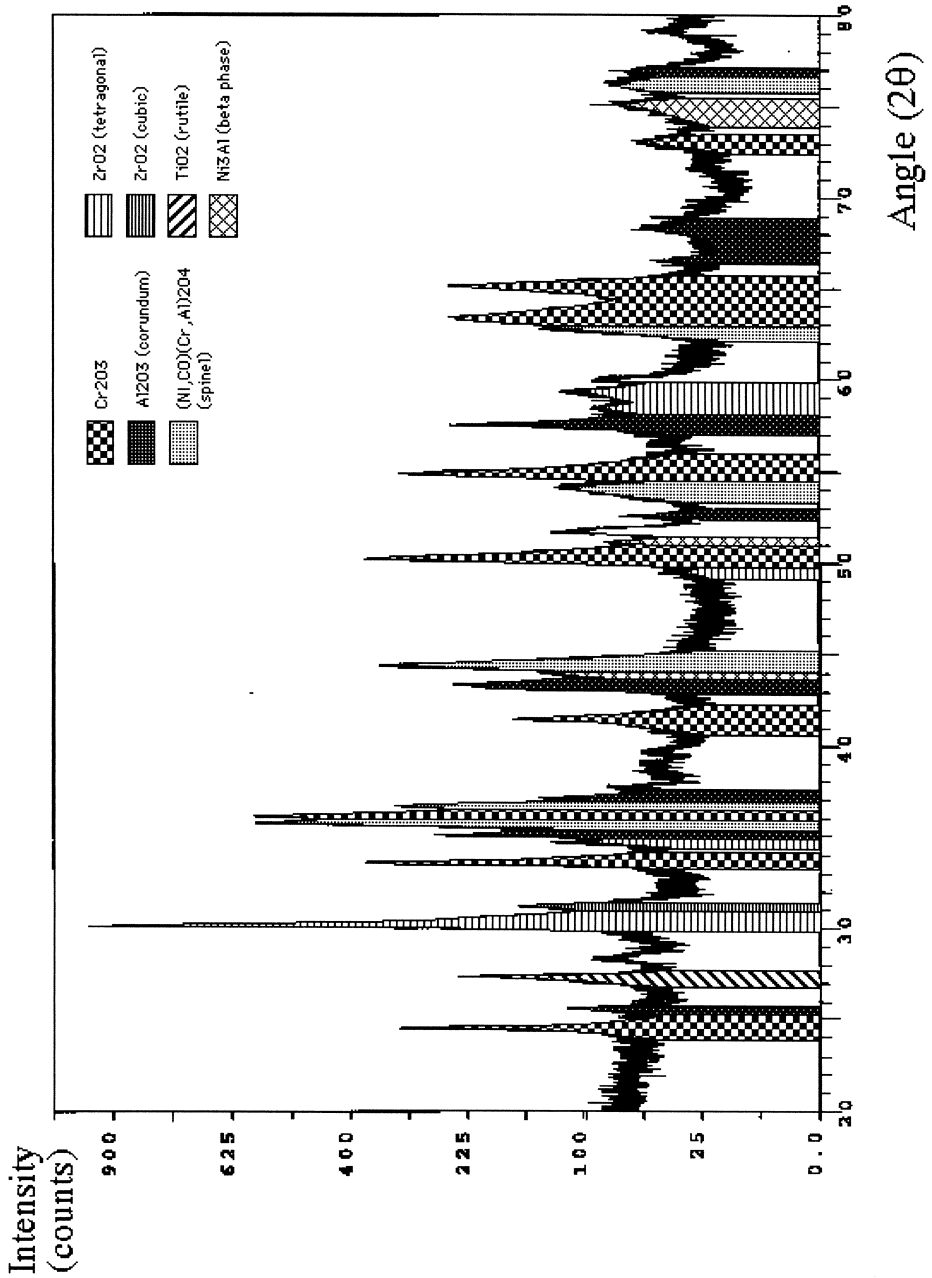

Fig. 6. X-ray diffraction data from the surface exposed by spalling of the TBC. As indicated the majority of peaks correspond to α-Cr_2O_3 with weaker peaks from a spinel phase, alumina and rutile. The zirconia is from the small fragments of TBC remaining attached to the bond-coat.

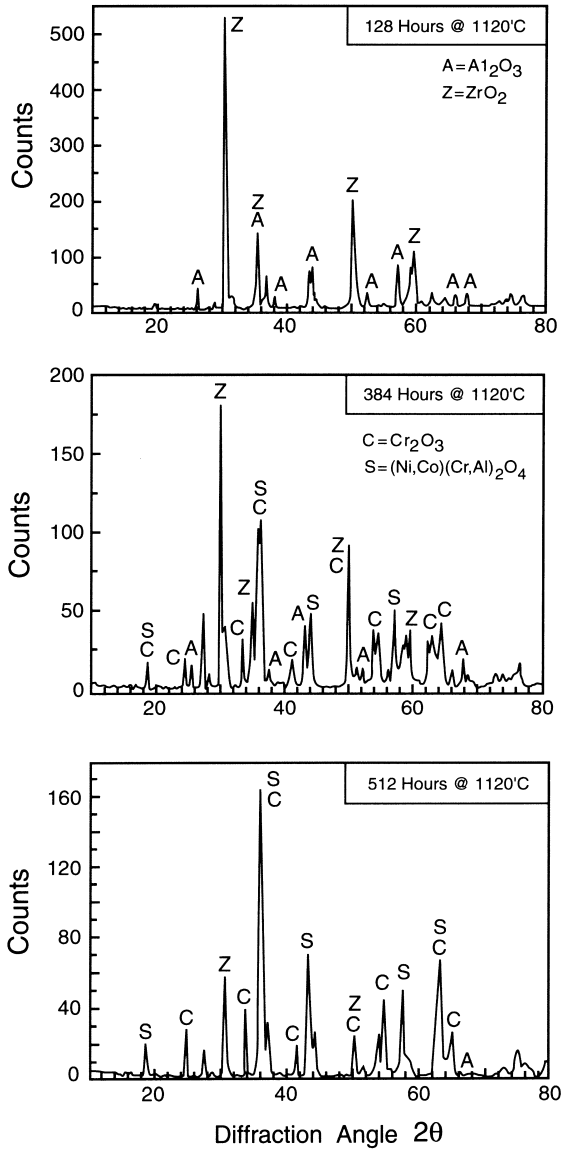

Fig. 7. X-ray diffraction data from the oxidized bond-coat surface for the oxidation times indicated. In each case, the TBC had been pried off to make the measurements.

sectioned and the phases in the oxide characterized on both the free surface and in the cross-section. After 128 h, the only phase detectable by X-ray diffraction (Fig. 7) and microscopy (Fig. 8) was α-alumina, as expected from the photoluminescence observations. (The peak from zirconia was from pieces of the zirconia coating still remaining after removing the bulk of the TBC.) After 256 h oxidation, however, the first indications of the formation of the spinel and α-chromia were detected on the surface by X-ray diffraction and in the cross-section by optical microscopy. These two phases became successively more pronounced with further oxidation exposure until, as shown in Fig. 7, alumina was no longer detectable by X-ray diffraction from the free surface after 512 h. This finding was in agreement with the observations of the spalled surface (Fig. 6). Additionally, the alumina phase was no longer continuous after 384 h oxidation and the oxide was principally a mixture of the (Co,Ni)(Cr,Al) spinel and α-chromia. Furthermore, "veins" of alumina, identified by their characteristic photoluminescence, appeared in the bond-coat alloy indicating that alumina was forming by internal oxidation rather than at the oxide surface (Fig. 8). Isolated alumina particles within the thermally grown mixed oxide could also be detected by their photoluminescence but were difficult to distinguish in the optical micrograph. Longer oxidation served to thicken the mixed oxide layer as well as increase the depth into the bond-coat where the alumina formed by internal oxidation.

5. DISCUSSION

The principal finding of this work is that spontaneous failure of the TBC occurred on cooling once the thermally grown oxide had converted from an initially continuous alumina scale to a mixed chromia, spinel scale. The delamination failure, presumably driven in by the increasing strain energy from the edge of the wedge-shaped TBC, suggests that the interfacial fracture resistances of the TBC/α-Cr_2O_3 and the TBC/spinel interfaces are lower than that of the TBC/α-Al_2O_3 interface originally present. This finding then raises the question as to the reason for the oxide phase conversion. Under equilibrium conditions, it is difficult to understand why an initially continuous, and presumably protective, alumina scale is replaced by the formation of α-chromia and spinel since alumina is the thermodynamically more stable oxide. As pointed out by Petit [12] those phases can form *below* the alumina scale once the activity of aluminum in the bond-coat has fallen below that necessary to form more alumina at the interface. However, they do not disrupt the alumina scale. One possibility is that the same process occurs as in breakaway oxidation of alloys [2]. In this scenario, prompted by thermal cycling, the alumina coating on the highly convoluted bond-coat surface cracks on cooling as a result of the high local curvatures and thermal expansion mismatch. Such cracks would, on heating back to the oxidation temperature, provide a direct transport path through the alumina for oxygen to react with the bond-coat and maintain a high partial pressure of oxygen at the interface. If, as is usually the case in high aluminum containing alloys, the bond-coat contains sufficient aluminum, more alumina will form and re-establish the protective film. However, if the alloy is locally depleted of aluminum, the other oxides can form. If the large volumetric change associated with the formation of these oxides is constrained, as it is likely to be by the overlying TBC, then this can lead to further

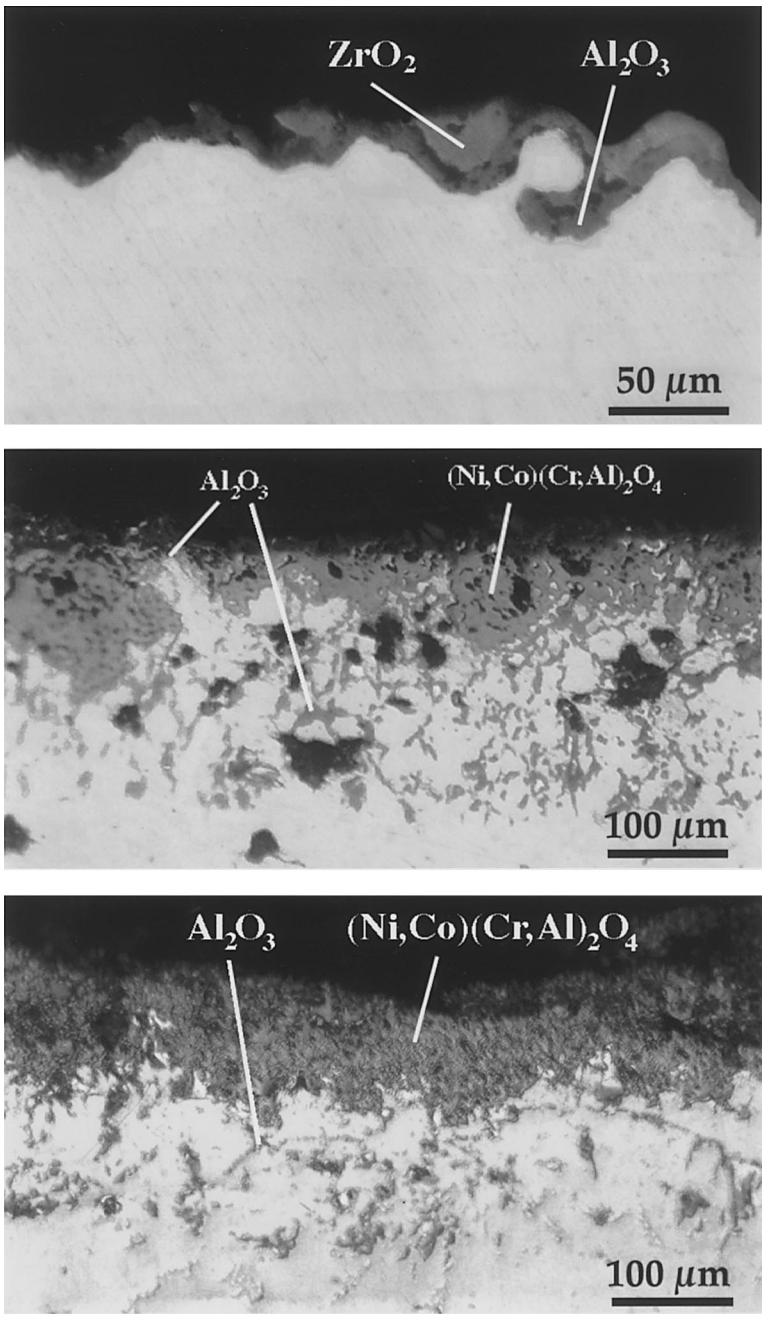

Fig. 8. Cross-section of the thermally grown oxide formed on the bond-coat after 128 h (top), 384 h (middle) and 512 h (bottom). Optical micrographs.

cracking of the alumina thereby further enhancing the formation of chromia and spinel. Without a protective scale, oxygen can diffuse well into the bond-coat alloy and form alumina by internal oxidation, as is observed.

The formation of Cr_2O_3 also provides an explanation for the unusual dependence of the apparent residual stress in the thermally grown alumina on oxidation time. As oxidation proceeds, the compressive stress in the alumina under the TBC increases over short times and then remains essentially unchanged for about 100 h at 1121°C. In this respect, the evolution in residual stress in the thermally grown oxide is similar to that seen on the oxidation of NiAl [13], Ni_3Al [14] and of TBC coated N5 superalloy with a PtAl bond-coat [15]. However, in contrast to the behavior of those alloys, the apparent compressive stress, shown in Fig. 2, then decreases with continued oxidation. The decrease coincides with the observed formation of Cr_2O_3 and is consistent with an increase in chromium concentration in the α-alumina phase. Also, since Cr_2O_3 is a strong absorber of the photostimulated Cr^{3+} luminescence, its formation may also be

responsible for the decrease in luminescence intensity observed after about 100 h. In fact, this suggests that the intensity of the photostimulated luminescence could be used as the basis for a non-destructive technique for monitoring the stability of the protective alumina scale. Although several factors influence the luminescence intensity, the intensity generally increases with thickness of the alumina scale and provided any chromia formed is beneath the alumina it does not affect the luminescence intensity from the alumina scale. However, when the volume of alumina decreases, for instance by dissolution to form spinel, or chromia forms above the alumina scale, the luminescence intensity will decrease. Furthermore, once the chromia layer completely covers the alumina, the intensity falls to zero. (This is the reason the alumina formed by internal oxidation could be detected in the polished cross-section but not through the mixed oxide scale from above.)

Finally, although Al depletion-based spalling was found to occur in only ~512 h it should be borne in mind that the oxidation temperature used (1121°C) is considerably higher than that to which this particular alloy/bond-coat/TBC combination would normally be exposed, or indeed is probably designed for. However, what was, in essence, an accelerated, high temperature test, does highlight the need for sufficient Al content in the bond-coat and underlying alloy to compensate for Al depletion during oxidation. This is especially important for the MCrAl bond-coats since there is sufficient Cr, Ni and Co in many of these bond-coats to shift the composition of the thermally grown oxide from Al_2O_3 to one of the other oxides over a prolonged time. Further experiments are underway to quantify the kinetics of this behavior.

6. CONCLUSIONS

Spalling of a plasma-sprayed thermal barrier coating from a 38Co–32Ni–21Cr–8Al–0.8Y bond-coated superalloy is found to occur at the interface between the thermally grown oxide and the zirconia TBC after 512 h at 1121°C. Luminescence and X-ray characterization indicate that the spalling is associated with the formation of a (Co,Ni)(Cr,Al) spinel and α-chromia, replacing the initially formed α-alumina thermally grown oxide in contact with the TBC. It is proposed that this phase conversion occurs, after thermal cycle induced cracking of the TGO, as a result of depletion of Al and enrichment of Co, Ni and Cr from the bond-coat alloy as oxidation proceeds.

Acknowledgements—This work was partially supported by the Advanced Gas Turbine Systems Research (AGTSR) program of the Department of Energy. The authors are grateful for discussions with V. Tolpygo throughout the course of this work.

REFERENCES

1. Whittle, D. P., Evans, D. J., Scully, D. B. and Wood, G. C., *Acta metall.*, 1967, **15**, 1412.
2. Hindam, H. and Whittle, D. P., *Oxidation Metals*, 1982, **18**, 245.
3. Nesbitt, J. A. and Heckel, R. W., *Oxidation Metals*, 1988, **29**(1/2), 75.
4. Mutasim, Z., Rimlinger, C. and Brentnall, W., Characterization of plasma sprayed and electron beam-physical vapor deposited thermal barrier coatings. American Society of Mechanical Engineers Publication 97-GT-531, 1997.
5. Ma, Q. and Clarke, D. R., *J. Am. Ceram. Soc.*, 1993, **76**(6), 1433.
6. Ma, Q. and Clarke, D. R., *J. Am. Ceram. Soc.*, 1994, **77**(2), 298.
7. Lipkin, D. M. and Clarke, D. R., *J. appl. Phys.*, 1995, **77**(5), 1855.
8. Lipkin, D. M. and Clarke, D. R., *Oxidation Metals*, 1996, **45**(3/4), 267.
9. He, J. and Clarke, D. R., *J. Am. Ceram. Soc.*, 1995, **78**(5), 1347.
10. Gong, X.-Y. and Clarke, D. R., *Oxidation Metals*, 1998, **50**(5/6), 355.
11. Kaplyanskii, A. A., Przhevuskii, A. K. and Rozenbaum, R. B., *Soviet Phys. Solid St.*, 1969, **10**, 1864.
12. Petit, F., 1996, Private communication.
13. Lipkin, D. M., Clarke, D. R., Hollatz, M., Bobeth, M. and Pompe, W., *Corros. Sci.*, 1997, **39**(2), 231.
14. Christensen, R. J., Lipkin, D. M. and Clarke, D. R., *Acta mater.*, 1996, **44**(9), 3813.
15. Christensen, R. J., Lipkin, D. M., Clarke, D. R. and Murphy, K., *Appl. Phys. Lett.*, 1996, **69**(24), 3754.